

Spin dynamics in stripe-ordered $\text{La}_{5/3}\text{Sr}_{1/3}\text{NiO}_4$ A. T. Boothroyd,^{1,*} D. Prabhakaran,¹ P. G. Freeman,¹ S. J. S. Lister,^{1,†} M. Enderle,² A. Hiess,² and J. Kulda²¹*Department of Physics, Oxford University, Oxford OX1 3PU, United Kingdom*²*Institut Laue-Langevin, BP 156, 38042 Grenoble Cedex 9, France*

(Received 29 January 2003; published 28 March 2003)

Polarized- and unpolarized-neutron inelastic scattering has been used to measure the spin excitations in the striped spin-charge-ordered phase of $\text{La}_{5/3}\text{Sr}_{1/3}\text{NiO}_4$. Above 30 meV, sharp magnetic modes are observed characteristic of a static stripe lattice. This part of the energy spectrum is described well by a linear spin-wave model with intrastripe and interstripe exchange interactions between neighboring Ni spins given by $J = 15 \pm 1.5$ meV and $J' = 7.5 \pm 1.5$ meV, respectively. A pronounced suppression and broadening of the magnetic fluctuations in a band between 10 meV and 25 meV is suggestive of coupling to collective motions of the stripe domain walls.

DOI: 10.1103/PhysRevB.67.100407

PACS number(s): 75.30.Ds, 71.45.Lr, 75.30.Et, 75.30.Fv

Over the past decade, the tendency for doped antiferromagnetic oxides to exhibit ordered phases involving both spin and charge has become increasingly apparent. Widespread interest was generated by the discovery of a striped spin-charge-ordered phase in a nonsuperconducting layered cuprate.¹ This stripe phase, the like of which has now been found in many other doped transition-metal oxide systems, is characterized by parallel lines of holes that act as charged domain walls separating regions of antiferromagnetically ordered spins. Its discovery fuelled a debate about the role played by stripe correlations in the superconducting state in the cuprates,² and stimulated numerous experimental investigations into stripe phenomena. These have focused principally on the $\text{La}_{2-x}\text{Sr}_x\text{NiO}_{4+\delta}$ series, which exhibits stripe ordering over a wide range of hole concentration.^{3,4}

Whereas the static properties of stripe-ordered phases are now quite well characterized, less is known about their dynamics. Specifically, there is a lack of information on how the collective motions of the holes in a stripe domain wall couple to the spin dynamics of the antiferromagnetic domains. One way to make progress in understanding stripe dynamics is to use neutron inelastic scattering to probe the spin excitation spectrum as a function of wave vector and energy in simple compounds exhibiting well-correlated stripe ordering. As well as providing information on the microscopic interactions that govern the properties of stripes, such studies can address the question of whether stripes are essential or incidental to the mechanism of superconductivity.

Here we report polarized- and unpolarized-neutron-scattering measurements of the spin excitation spectrum in the ordered-stripe phase of $\text{La}_{5/3}\text{Sr}_{1/3}\text{NiO}_4$. This composition has not been studied before by neutron inelastic scattering, and was chosen because the spin-charge order is particularly well correlated and has a very simple superstructure commensurate with the crystal lattice^{4,7-9}—see Fig. 1(a). Compared with other neutron-scattering studies of stripe-ordered $\text{La}_{2-x}\text{Sr}_x\text{NiO}_{4+\delta}$ compounds,^{5,6} our measurements cover a wider range of wave vector and energy than previously explored in any one compound, and the simplicity of the magnetic structure of $\text{La}_{5/3}\text{Sr}_{1/3}\text{NiO}_4$ allows us to compare the data with a simple spin-wave model. Thus, we determine values for the nearest-neighbor coupling strengths for spins

within a stripe domain and for spins separated by a charged domain wall. We also observe features in the magnetic scattering between 10 meV and 25 meV, which could, we suggest, originate from coupling between spin excitations and collective motions of the charged domain walls.

Two single crystals of $\text{La}_{5/3}\text{Sr}_{1/3}\text{NiO}_4$ in the form of rods, 7–8 mm in diameter and ~ 40 mm in length, were used for the experiments. Both were grown from the same batch of starting powder by the floating-zone method.¹⁰ Their oxygen excess was determined by thermogravimetric analysis to be $\delta = 0.01 \pm 0.01$, and their electrical and magnetic properties were found to be in very good agreement with data in the literature.⁷

Neutron inelastic scattering measurements were performed on the IN20 and IN22 triple-axis spectrometers at the

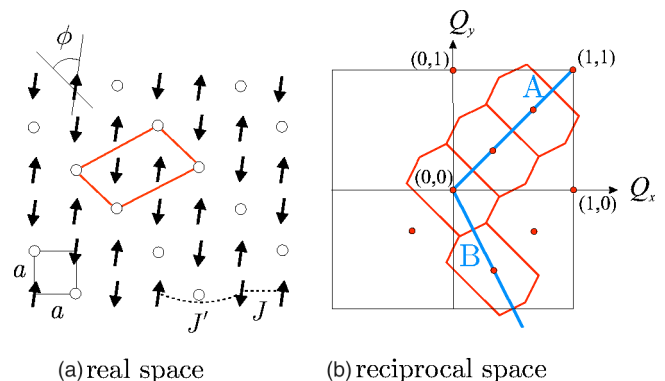


FIG. 1. (Color online) (a) Model for the stripe order found in the NiO_2 plane of $\text{La}_{5/3}\text{Sr}_{1/3}\text{NiO}_4$ (Refs. 4 and 9). Arrows denote $S = 1$ spins on the Ni^{2+} sites, open circles represent Ni^{3+} holes. The O sites are not shown. ϕ is the angle between the spin axes and the stripe direction. Primitive unit cells of the NiO_2 square lattice and stripe superstructure are indicated, respectively, by the small square and parallelogram. J and J' are intrastripe and interstripe exchange interactions between nearest-neighbor Ni spins. (b) Diagram of reciprocal space showing several Brillouin zones for the stripe superlattice shown in (a). The (h,k) indices refer to the NiO_2 square lattice, and the small circles are the stripe superlattice zone centers. The lines marked A and B indicate the scan directions used in the experiment.

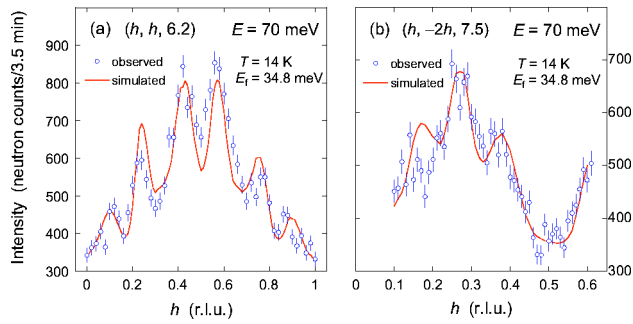


FIG. 2. (Color online) \mathbf{Q} scans parallel to (a) $(h, h, 0)$ and (b) $(h, -2h, 0)$ at a constant energy of 70 meV, showing the magnetic scattering from $\text{La}_{5/3}\text{Sr}_{1/3}\text{NiO}_4$. The lines are simulations of the scans generated by convolution of the calculated spectrometer resolution with the spin-wave model discussed in the text.

Institut Laue-Langevin. The incident and final neutron energies were selected by Bragg reflection from an array of either pyrolytic graphite (PG) or Heusler alloy crystals, depending on whether unpolarized or polarized neutrons were employed. Scans were performed with a fixed final energy of either $E_f = 14.7$ meV or 34.8 meV, and a PG filter was present to suppress higher-order harmonics in the scattered beam. Two settings of the crystal were used, giving access to the (h, h, l) and $(h, -2h, l)$ planes in reciprocal space. In this paper, the reciprocal lattice is indexed with respect to a body-centered tetragonal lattice with cell parameters $a = 3.8$ Å and $c = 12.7$ Å.

Long-range ordering of holes and spins in $\text{La}_{5/3}\text{Sr}_{1/3}\text{NiO}_4$ occurs below $T_{\text{CO}} \approx 240$ K and $T_{\text{SO}} \approx 200$ K, respectively. The stripe arrangement formed in the Ni-O layers is shown in Fig. 1(a).^{4,9} The spins are collinear, and ϕ is the angle between the spin axes and the stripe direction. All the measurements reported here were taken at $T = 14$ K, at which temperature $\phi = 53^\circ$ and the in-plane and out-of-plane spin and charge-order correlation lengths are several hundred angstroms and 20–50 Å, respectively.^{4,8} In inelastic measurements the c -axis correlations were found to decay very rapidly with energy, entirely disappearing above 5 meV. Over the energy range considered here, it is therefore reasonable to treat the spin dynamics as two dimensional.

Figure 1(b) shows several two-dimensional Brillouin zones of the stripe order. We probed the excitation spectrum either by scanning the neutron-scattering vector \mathbf{Q} along the lines marked *A* and *B* at a fixed energy, or by scanning the energy at a fixed \mathbf{Q} . In reality, the ordered-stripe phase contains equal proportions of two twins with stripes at 90° to one another. The reciprocal space for the second twin is rotated by 90° with respect to that shown in Fig. 1(b). Experimentally, one observes a superposition of the scattering from both twins.

Assuming the ordered ground state in Fig. 1, one expects to observe magnetic excitations dispersing from the magnetic zone centers, and indeed this is confirmed by our measurements. To illustrate the results, Fig. 2 shows wave-vector scans parallel to the $(h, h, 0)$ and $(h, -2h, 0)$ directions measured with unpolarized neutrons at a fixed energy of 70 meV. The six peaks observed in Fig. 2(a) correspond to spin exci-

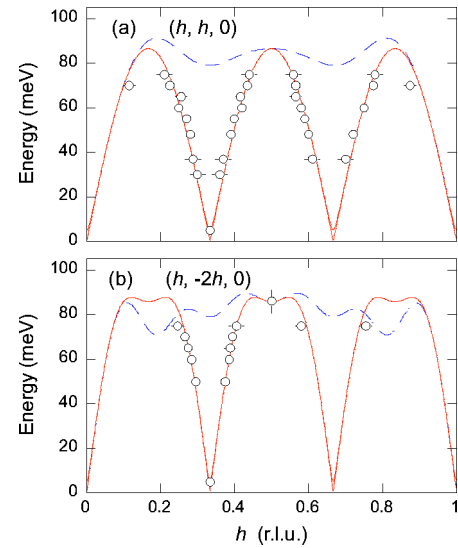


FIG. 3. (Color online) Dispersion of the magnetic excitations in $\text{La}_{5/3}\text{Sr}_{1/3}\text{NiO}_4$ parallel to (a) $(h, h, 0)$ and (b) $(h, -2h, 0)$. The full and broken lines are the spin-wave model dispersion for the two twins [Eq. (1)], calculated with parameters $J = 15$ meV, $J' = 7.5$ meV, and $K_c = 0.07$ meV.

tations propagating in a direction perpendicular to the stripes away from successive zone centers along the *A* line in Fig. 1(b). Similarly, the two strongest peaks in Fig. 2(b) are spin excitations propagating away from $(1/3, -2/3)$ along line *B*, approximately parallel to the stripes. Under the experimental conditions used, we were not able to resolve the separate peaks associated with each zone center when the energy was below 37 meV.

In Fig. 3, we plot the dispersion of the spin excitations along the $(h, h, 0)$ and $(h, -2h, 0)$ directions as deduced from a series of (mainly) constant-energy scans like those of Fig. 2. To arrive at the data points shown in Fig. 3, we corrected the observed peak positions for small shifts (10–20%) caused by the spectrometer resolution as it intersects the curved dispersion surface. We determined the corrections by convolution of the resolution function with the model dispersion surface to be described later.

In the energy range 10–30 meV, very strong scattering from phonons makes it difficult to identify unambiguously the magnetic scattering with unpolarized neutrons. Therefore, to explore this energy range we employed polarization analysis, keeping the neutron polarization direction \mathbf{P} parallel to \mathbf{Q} . In this configuration the neutron spins are flipped when scattered by magnetic excitations, but remain unchanged in nonmagnetic (e.g., phonon) scattering processes. The measured flipping ratio of ~ 20 was used to correct for nonideal polarization.

Figure 4(a) shows the neutron spin-flip (SF) and non-spin-flip (NSF) scattering observed as a function of energy with \mathbf{Q} fixed at the $(4/3, 4/3, 0)$ magnetic zone center. The separation of the magnetic and nonmagnetic scattering by the polarization analysis is exemplified by the sharp phonon peaks centered on 16.5 meV and 22 meV in the NSF channel, which are not present in the SF channel. However, the most remarkable feature in this scan is the broad valley centered near 15

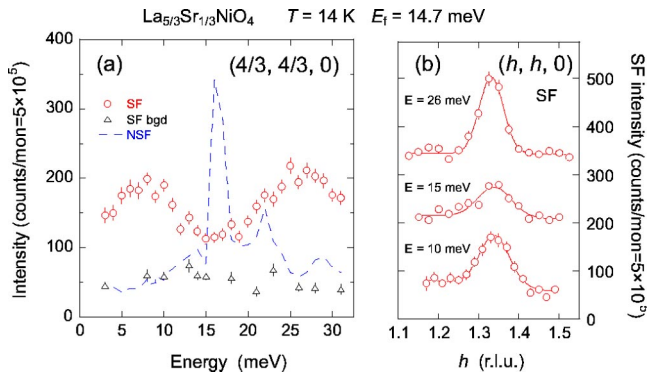


FIG. 4. (Color online) (a) Spin-flip (SF) and non-spin-flip (NSF) scattering as a function of energy at a constant wave vector of $(4/3, 4/3, 0)$. The sharp peaks in the NSF channel are due to phonons. The SF background is estimated from data collected at $(1.2, 1.2, 0)$. (b) SF scattering intensity plotted as a function of wave vector for energies of 10 meV, 15 meV, and 26 meV. The upper two scans have been shifted vertically by 150 and 300 counts, respectively. The lines are fits to a single Gaussian peak profile.

meV in the SF scattering. By comparison with the SF measurements made at $\mathbf{Q} = (1.2, 1.2, 0)$, where the magnetic scattering has decreased to background level, we see that the amplitude of the magnetic signal above background is nearly a factor 3 smaller at $E = 15$ meV than at either $E = 10$ meV or $E = 26$ meV. Similar scans measured at $(1/3, 1/3, l)$, $l = 4.5, 5.5$, show the same valley feature. A secondary feature observed in Fig. 4(a) is the drop in magnetic intensity with decreasing energy below ~ 7 meV.

One possible origin for the features just described could be spin anisotropy gaps. Below an anisotropy gap a component of the spin fluctuations freezes out, causing a reduction in scattering intensity. We checked this possibility by comparing the magnetic scattering intensities for neutron polarizations $\mathbf{P} \parallel \mathbf{Q}$ and $\mathbf{P} \perp \mathbf{Q}$. The data at 10 meV, 15 meV, and 26 meV were all consistent with the assumption of isotropic transverse spin fluctuations about the direction of the ordered moment. At 3 meV, however, the signal is predominantly due to in-plane transverse spin fluctuations. Therefore, we conclude that the drop in intensity below ~ 7 meV is caused by an out-of-plane anisotropy gap, but that the main valley feature cannot be explained by spin anisotropy.

Figure 4(b) shows the SF scattering intensity measured in a series of constant-energy scans in the neighborhood of the valley feature. These data show that, in addition to a reduction in amplitude, there is also an increase in width. The 15-meV peak is found to be $\sim 50\%$ broader in wave vector than the 10-meV and 26-meV peaks. This broadening suggests that the valley feature is associated with the decay of antiferromagnetic spin excitation modes through hybridization with another type of excitation. One possibility is a coupling to optic phonons intrinsic to the material, but we do not believe this to be the case because (i) the valley region is ~ 10 meV wide, much larger than the width of individual phonon excitations, and (ii) we do not observe any structure in the SF scattering channel due to the excitation of phonons through a magnetoelastic interaction.

Having established the overall features of the spin excitation spectrum, we next consider a simple model to help interpret the results and to estimate the principal exchange constants. The data above 30 meV exhibit sharp propagating modes with a dispersion consistent with the periodicity of the static stripe lattice (Fig. 1), and as a first approximation we therefore neglect the motion of the holes and consider the spin Hamiltonian

$$H = J \sum_{\langle ij \rangle} \mathbf{S}_i \cdot \mathbf{S}_j + J' \sum_{\langle ij' \rangle} \mathbf{S}_i \cdot \mathbf{S}_{j'} + K_c \sum_i (S_i^z)^2, \quad (1)$$

where the first two summations are over pairs of nearest-neighbor Ni spins, the first sum having both spins within the same stripe domain and the second having the two spins in adjacent domains separated by a line of holes. J and J' are the corresponding exchange parameters—see Fig. 1(a). The third term describes the out-of-plane anisotropy. The in-plane anisotropy is much smaller than the out-of-plane anisotropy and is neglected.

We used the linear spin-wave approximation to calculate the energy dispersion and scattering cross section from Eq. (1), and after convolving the model spectrum with the spectrometer resolution we compared the results with the measured scans. The parameters $J = 15 \pm 1.5$ meV, $J' = 7.5 \pm 1.5$ meV, and $K_c = 0.07 \pm 0.01$ meV gave the best description of the data. For reference, the J and K_c parameters obtained by Nakajima *et al.*¹¹ from a fit to the spin-wave dispersion of La_2NiO_4 were 15.5 meV and 0.52 meV, respectively. We find, therefore, that the spin anisotropy is strongly reduced in the doped compound, but the strength of the nearest-neighbor exchange interaction within an antiferromagnetic domain is essentially unaffected by hole doping.

The spin-wave model gives a good account of the spectrum above ~ 25 meV. For illustration, the lines drawn on Figs. 2(a) and 2(b) show scan simulations, and are seen to match the main features of the data quite well. The inclusion of more exchange parameters might achieve even better agreement, but is not justified given the extent of the present data set. We did, however, consider an alternative model in which the interdomain exchange J' couples pairs of spins displaced by (a, a) instead of $(2a, 0)$. However, the deviations from the first model were slight and mainly confined to energies close to the zone boundary energy where data are sparse. Hence, although the absolute values of the parameters may be subject to systematic errors due to the linear approximation and neglect of more distant couplings, we expect that the relative strengths of the intrastripe and interstripe spin couplings are reliably estimated by the present analysis.

On the other hand, the behavior observed in the energy range 10–25 meV represents a clear departure from the spin-wave model. The dip in magnetic scattering around 15 meV and accompanying increase in width are not reproduced in the scan simulations.

The results presented here provide several important insights into the dynamics of stripe phases. At high energies, the spin excitations propagate as if the underlying charge-ordered lattice were static. Assuming static stripes our analy-

sis has provided estimates for J and J' , and uncovered a dramatic reduction in single-ion spin anisotropy relative to La_2NiO_4 . Our high-energy data are consistent with those of Bourges *et al.*⁶ on $\text{La}_{1.69}\text{Sr}_{0.31}\text{NiO}_4$, but the advantage of the $\text{La}_{5/3}\text{Sr}_{1/3}\text{NiO}_4$ compound studied here is that its simple stripe superstructure is amenable to analysis by a microscopic model. Thus, Bourges *et al.* report a lack of anisotropy in the spin-wave velocity, but if measured by the ratio J/J' then we find the anisotropy in the spin coupling to be close to 2.

Concerning the behavior in the 10–25 meV range, we have ruled out the existence of spin anisotropy gaps and argued against coupling to intrinsic phonons as an explanation for the valley/broadening feature. Moreover, the scattering in this range is not complicated by the twinning. Instead, we suggest that this feature arises from the interaction between spin excitations and collective motions of the stripe domain walls. In support of this hypothesis, we note that the stripe-ordering temperature (~ 240 K) in this compound translates to ~ 20 meV. In other words, the thermal energy needed to destroy long-range order of the stripes is comparable to the energy where we observe the broadening in the spin excitations. Zaanen *et al.*¹² discussed the dynamics of charged domain-wall motion in an antiferromagnetic background on general theoretical grounds, and argued that domain-wall fluctuations will have their strongest influence on the spin excitation spectrum at low energies consistent

with our observations. It is interesting, however, that the broadening appears to be restricted to a band of energies below which the spin excitations sharpen again. A possible explanation is that there exists a commensurability gap of ~ 10 meV for domain-wall motions due to the pinning of the charges to the lattice. If this were the case, then one might expect the valley feature to be absent from the spin excitation spectrum of compounds whose stripe period is incommensurate with the lattice.

Finally, we draw attention to recent calculations of the imaginary parts of the charge and spin dynamical susceptibilities of an ordered-stripe system described by the Hubbard model.^{13,14} In addition to transverse spin waves, these calculations also predict longitudinal modes arising from meandering and compressive movements of the domain walls. We did not observe sharp phasonlike modes of the type predicted, but their weak intensity relative to the spin-wave scattering and the broadening in the valley region may have precluded their observation.

We thank L.-P. Regnault for help with the IN22 experiments, P. Isla, D. Gonzalez, and R. Burriel for sample characterization, and J. Zaanen and J. Chalker for stimulating discussions. A.T.B. is grateful to the Institut Laue-Langevin for support during a three-month visit in 2002. This work was supported by the Engineering & Physical Sciences Research Council of Great Britain.

*Electronic address: a.boothroyd1@physics.ox.ac.uk; URL: <http://xray.physics.ox.ac.uk/Boothroyd>

†Present address: Oxford Magnet Technology Ltd., Witney, Oxfordshire OX29 4BP, United Kingdom.

¹J.M. Tranquada *et al.*, Nature (London) **375**, 561 (1995).

²J. Zaanen and O. Gunnarsson, Phys. Rev. B **40**, 7391 (1989); K. Machida, Physica C **158**, 192 (1989); V.J. Emery and S.A. Kivelson, *ibid.* **209**, 597 (1993); J. Zaanen, Nature (London) **404**, 714 (2000).

³C.H. Chen, S-W. Cheong, and A.S. Cooper, Phys. Rev. Lett. **71**, 2461 (1993); J.M. Tranquada *et al.*, *ibid.* **73**, 1003 (1994).

⁴H. Yoshizawa *et al.*, Phys. Rev. B **61**, R854 (2000).

⁵S.M. Hayden *et al.*, Phys. Rev. Lett. **68**, 1061 (1992); J.M. Tranquada, P. Wochner, and D.J. Buttrey, *ibid.* **79**, 2133 (1997);

K. Nakajima and Y. Endoh, J. Phys. Soc. Jpn. **67**, 1552 (1998); S.-H. Lee *et al.*, Phys. Rev. Lett. **88**, 126401 (2002).

⁶P. Bourges *et al.*, cond-mat/0203187 (unpublished).

⁷S-W. Cheong *et al.*, Phys. Rev. B **49**, 7088 (1994).

⁸C-H. Du *et al.*, Phys. Rev. Lett. **84**, 3911 (2000).

⁹S.-H. Lee *et al.*, Phys. Rev. B **63**, 060405 (2001).

¹⁰D. Prabhakaran, P. Isla, and A.T. Boothroyd, J. Cryst. Growth **237**, 815 (2002).

¹¹K. Nakajima *et al.*, J. Phys. Soc. Jpn. **62**, 4438 (1993).

¹²J. Zaanen *et al.*, Phys. Rev. B **53**, 8671 (1996).

¹³E. Kaneshita, M. Ichioka, and K. Machida, J. Phys. Soc. Jpn. **70**, 866 (2001).

¹⁴S. Varlamov and G. Seibold, Phys. Rev. B **65**, 075109 (2002).